Electronic Supplementary Material (ESI) for Chemical Science

Supporting Information

Peptide-Intercalated Layered Metal Hydroxides: Effect of Peptide Chain Length and Side Chain Functionality on Structural, Optical and Magnetic Properties

*Satyabrata Si, (1, 2) Andreas Taubert, (3,4) Alexandre Mantion (5),Guillaume Rogez, (1), Pierre Rabu,(1)**

[1)] *IPCMS, UMR CNRS-UdS 7504, 23 rue du Loess, BP43, 67034 Strasbourg cedex 2, France*

[2)] *Functionalized Materials Group, ICMCB-University Bordeaux1, 87, Av. Dr Albert Schweitzer, 33608 PESSAC cedex, France*

[3)] *University of Potsdam, Institute of Chemistry, Karl-Liebknecht-Straße 24-25, 14476 Golm, Germany*

[4)] *MPI of Colloids and Interfaces, Am Mühlenberg 1, 14476 Golm, Germany*

[5)] *BAM, Federal Institute for Materials Research and Testing, Richard-Willstaetter-Str. 1, 12489 Berlin, Germany*

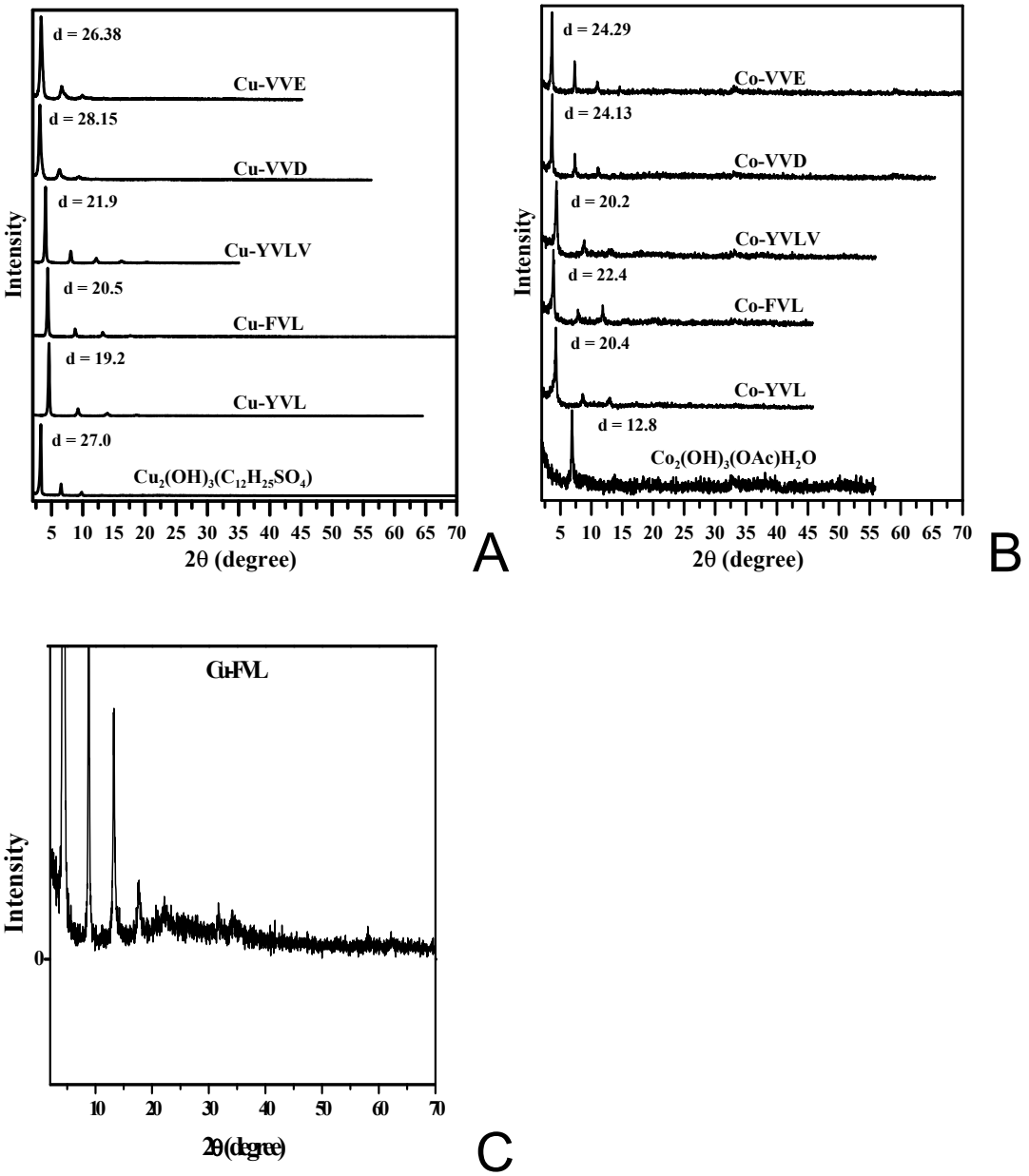

Figure S0: XRD patterns of the peptide grafted layered Cu(II) (A) and Co(II) hydroxides (B) showing the absence of significant diffraction lines above 30°. Sometimes, like in Cu-FVL (C) weak and broad lines are observed in the range 32-38 ° which can be assigned to hk0 planes. The numbers indicate the interlayer d spacing values in Å (001).

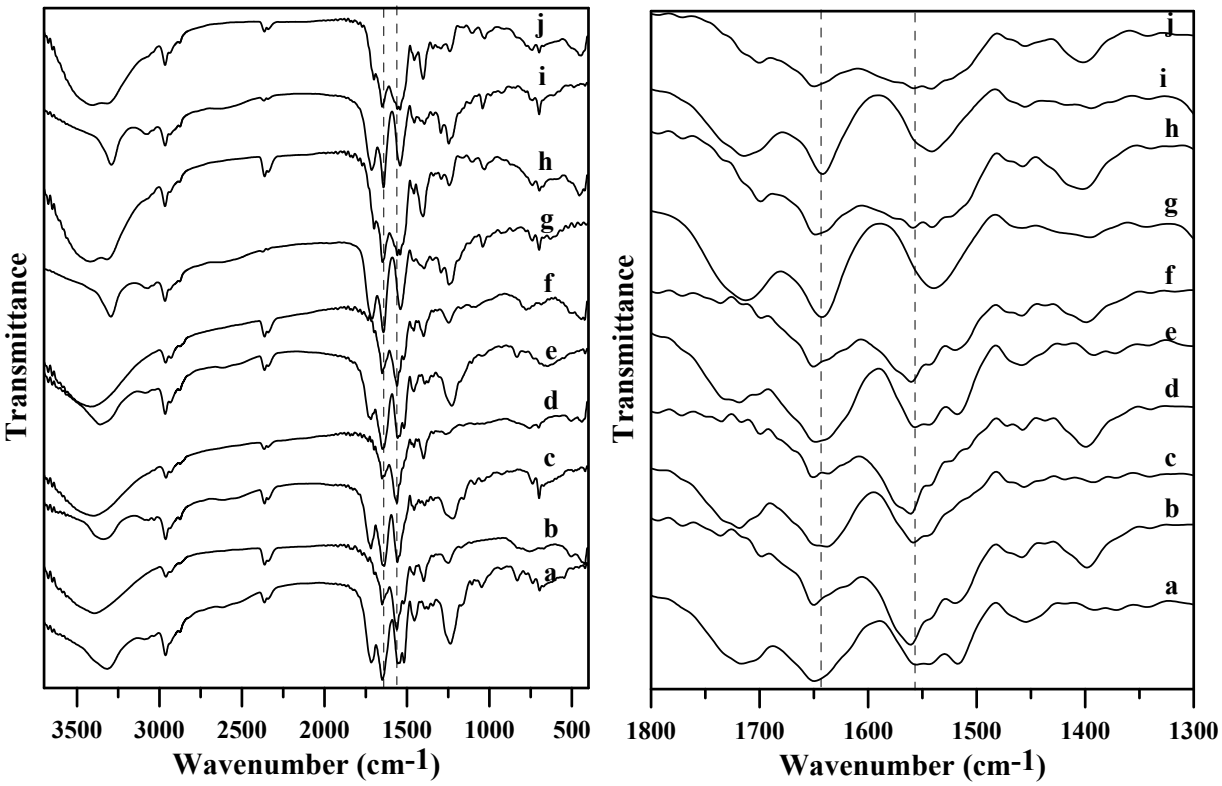

Figure S1: FTIR spectra of various peptides and their Cu-based hybrid; the enlarged view for the range 1800-1300 cm^{-1} is shown in the right side: (a) YVL, (b) Cu-YVL, (c) FVL, (d) Cu-FVL, (e) YVLV, (f) Cu-YVLV, (g) VVD, (h) Cu-VVD, (i) VVE, and (j) Cu-VVE.

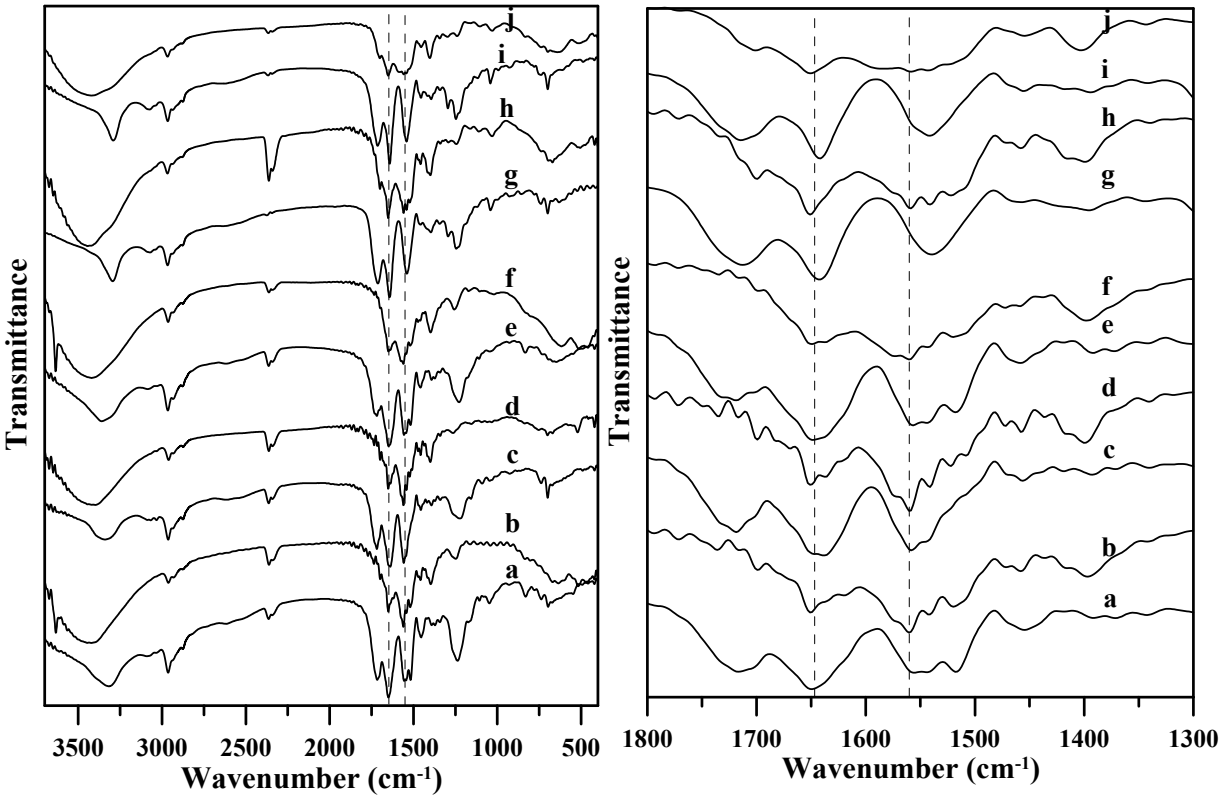

Figure S2: FTIR spectra of various peptides and their Co-based hybrid; the enlarged view for the range 1800-1300 cm^{-1} is shown in the right side: (a) YVL, (b) Co-YVL, (c) FVL, (d) Co-FVL, (e) YVLV, (f) Co-YVLV, (g) VVD, (h) Co-VVD, (i) VVE, and (j) Co-VVE.

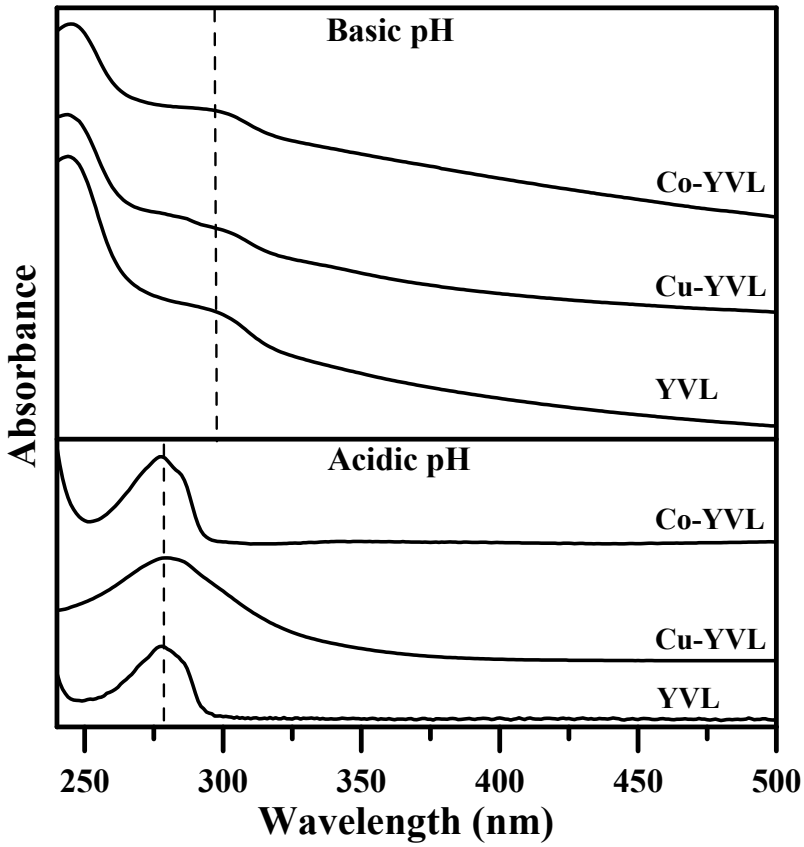

Figure S3: UV-vis absorption spectra of YVL, Cu-YVL and Co-YVL in acidic pH 3 and basic pH 9 (arbitrary absorbance units). The absorption band for Cu-YVL is broadened may be due the superimposition of tyrosine absorption and absorption due to the complex of the peptide with the dissolved Cu(II) ions.

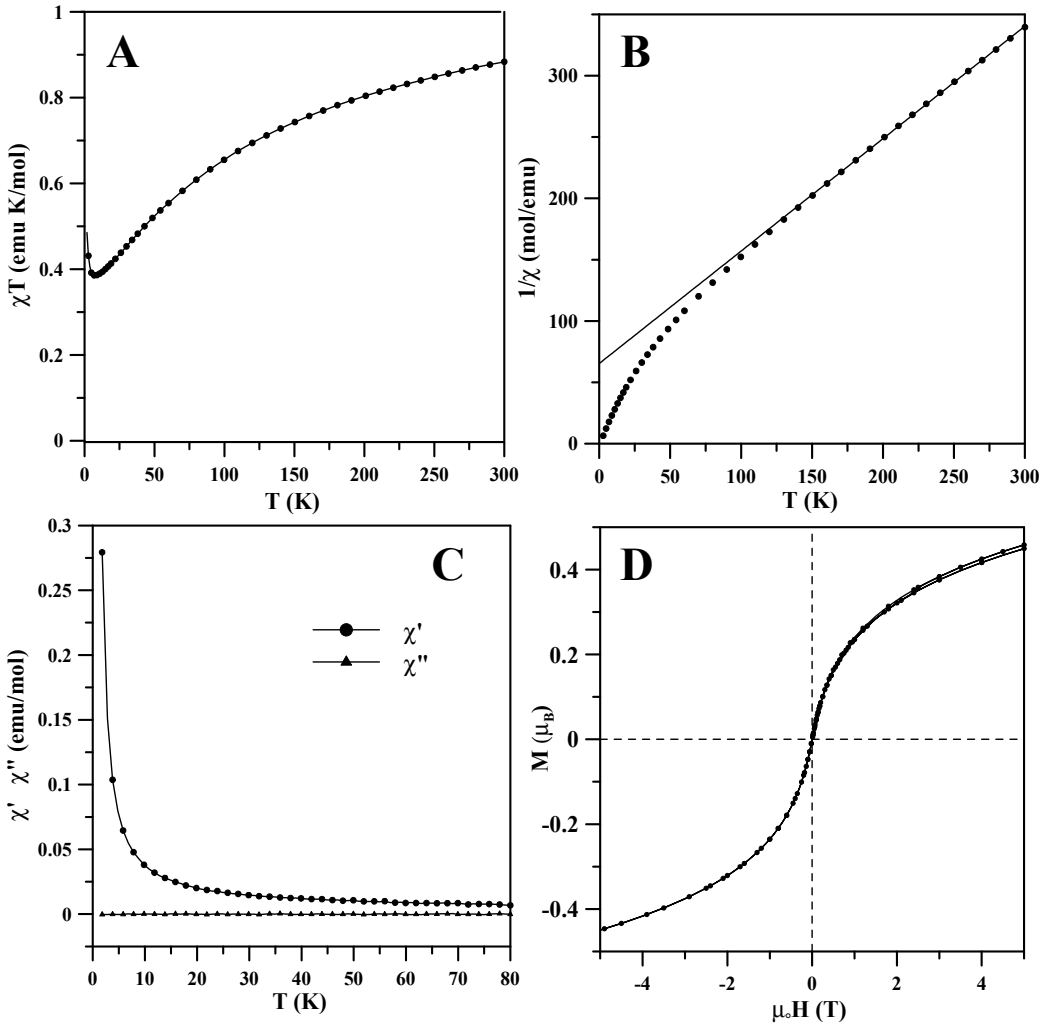

Figure S4: Magnetic characterization of the Cu-YVL hybrids: (A) χT as a function of temperature, (B) Inverse of χ as a function of temperature, (C) Magnetic susceptibility as a function of temperature in an ac field, and (D) Field dependant magnetization at 1.8 K.

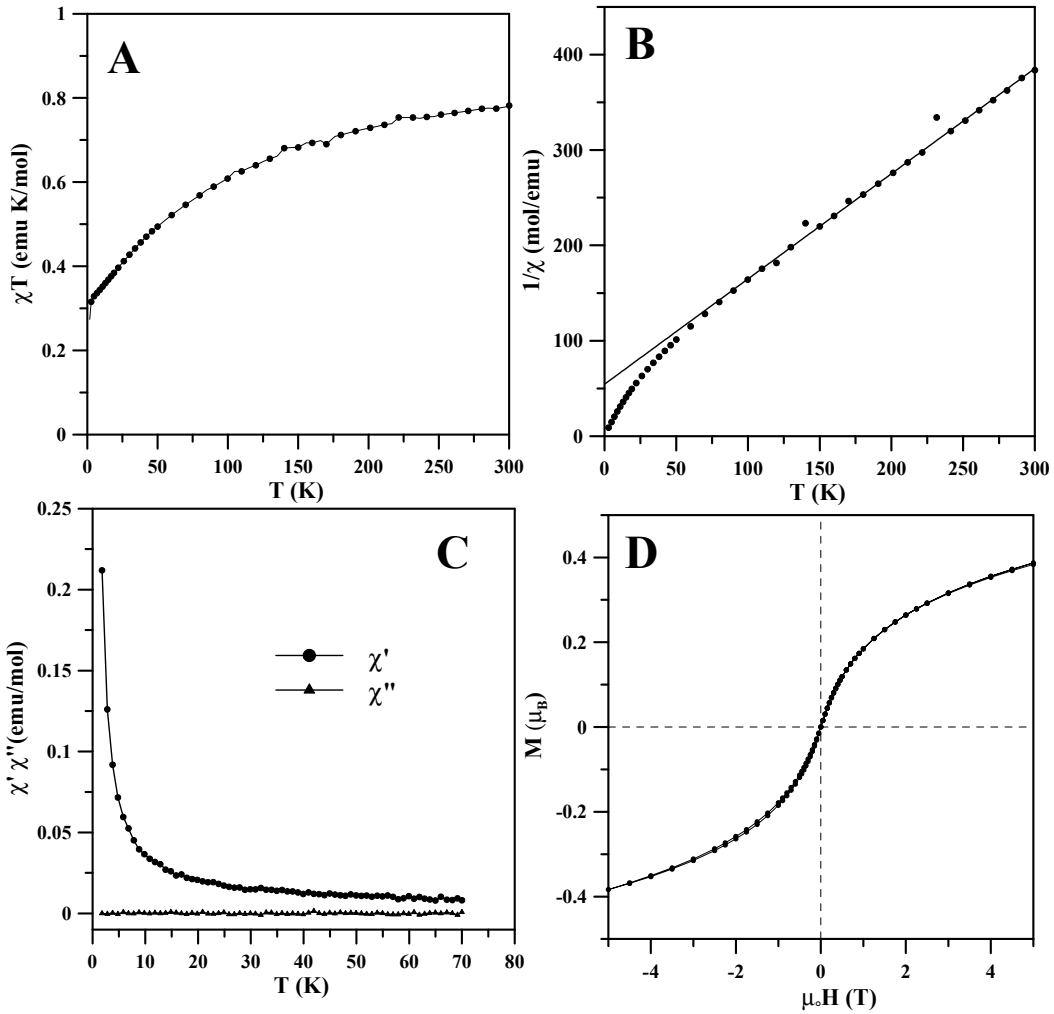

Figure S5: Magnetic characterization of the Cu-FVL hybrids: (A) χT as a function of temperature, (B) Inverse of χ as a function of temperature, (C) Magnetic susceptibility as a function of temperature in an ac field, and (D) Field dependant magnetization at 1.8K.

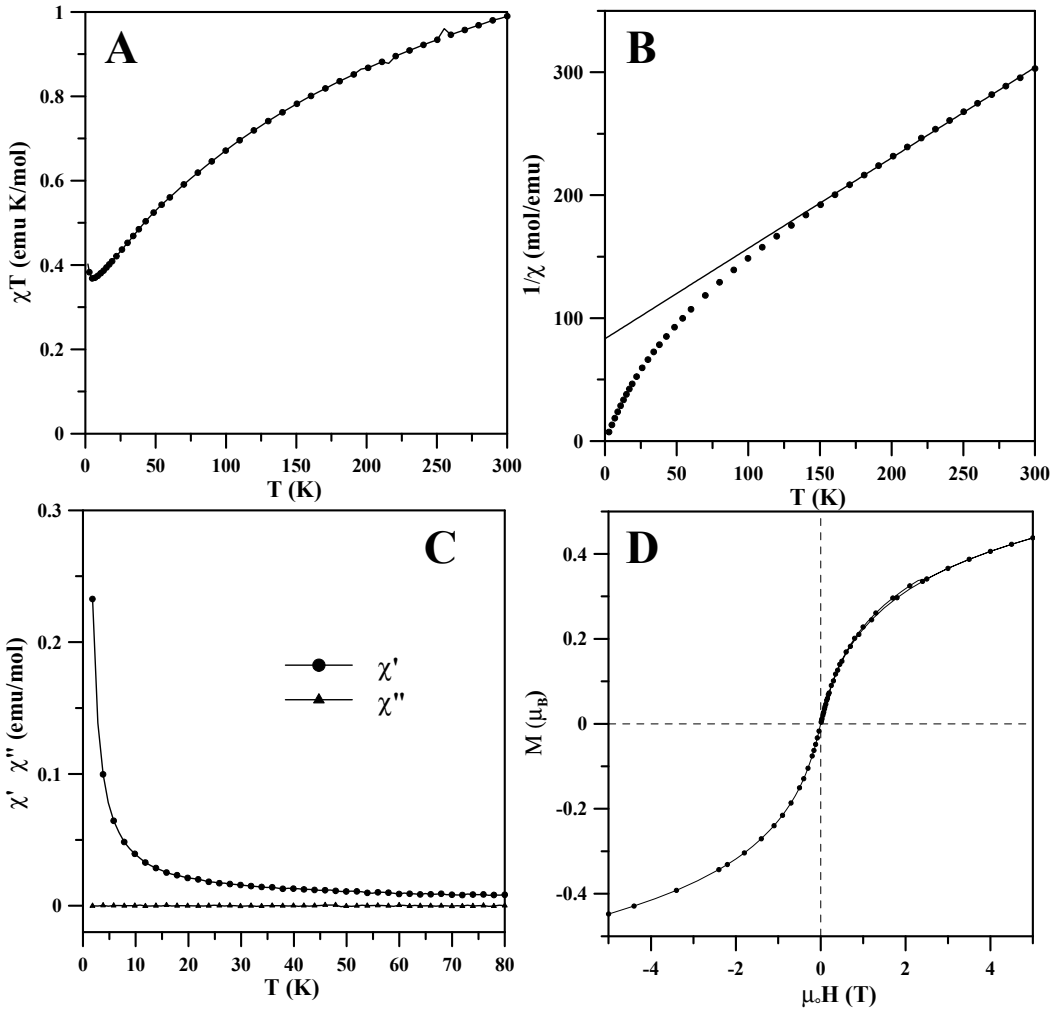

Figure S6: Magnetic characterization of the Cu-YVLV hybrids: (A) χT as a function of temperature, (B) Inverse of χ as a function of temperature, (C) Magnetic susceptibility as a function of temperature in an ac field, and (D) Field dependant magnetization at 1.8 K.

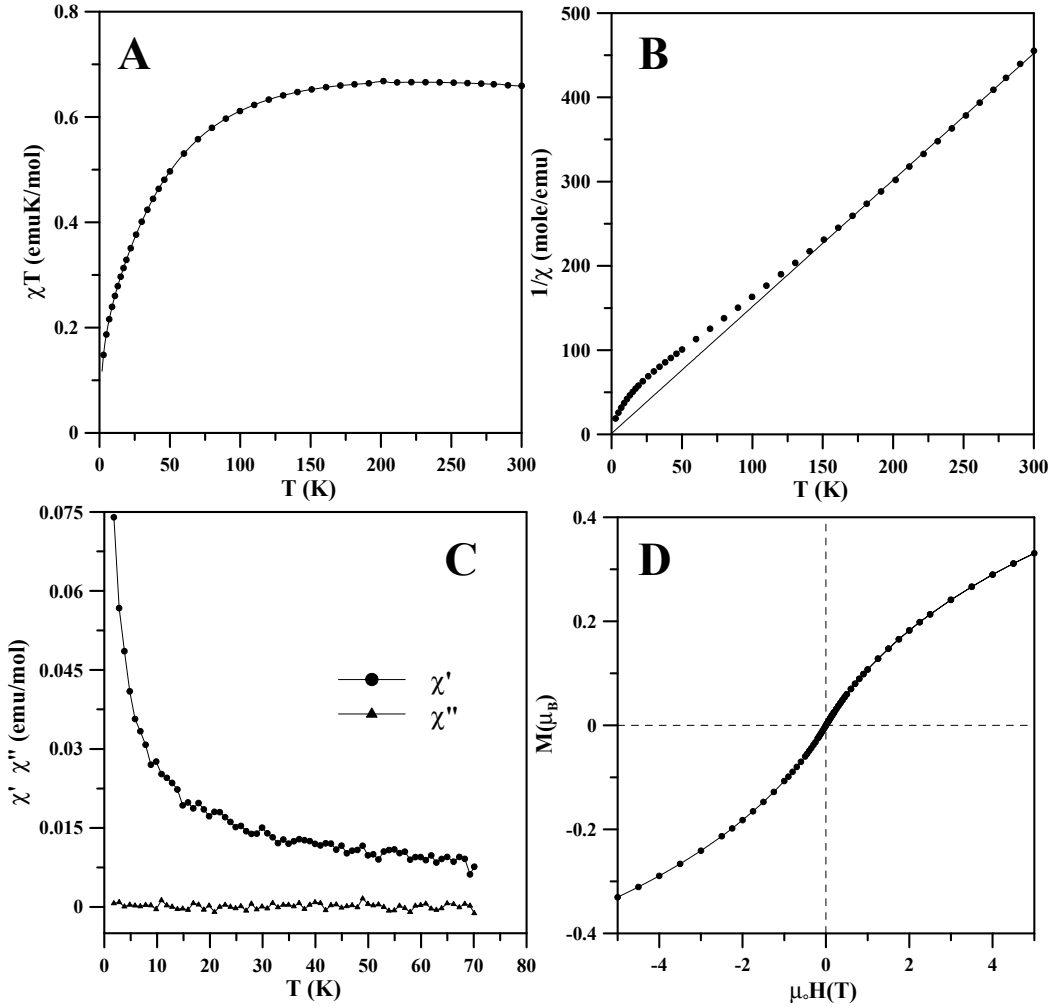

Figure S7: Magnetic characterization of the Cu-VVD hybrids: (A) χT as a function of temperature, (B) Inverse of χ as a function of temperature, (C) Magnetic susceptibility as a function of temperature in an ac field, and (D) Field dependant magnetization at 1.8 K.

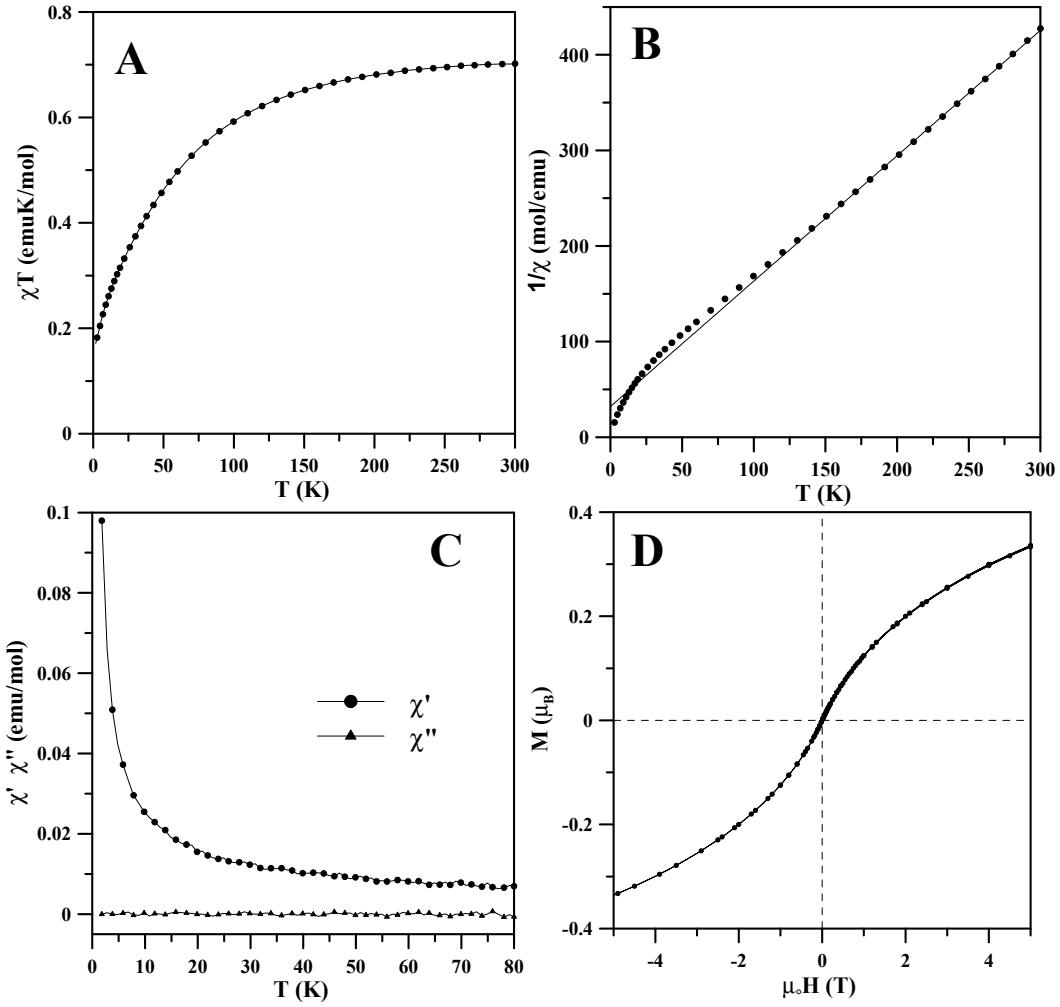

Figure S8: Magnetic characterization of the Cu-VVE hybrids: (A) χT as a function of temperature, (B) Inverse of χ as a function of temperature, (C) Magnetic susceptibility as a function of temperature in an ac field, and (D) Field dependant magnetization at 1.8 K..

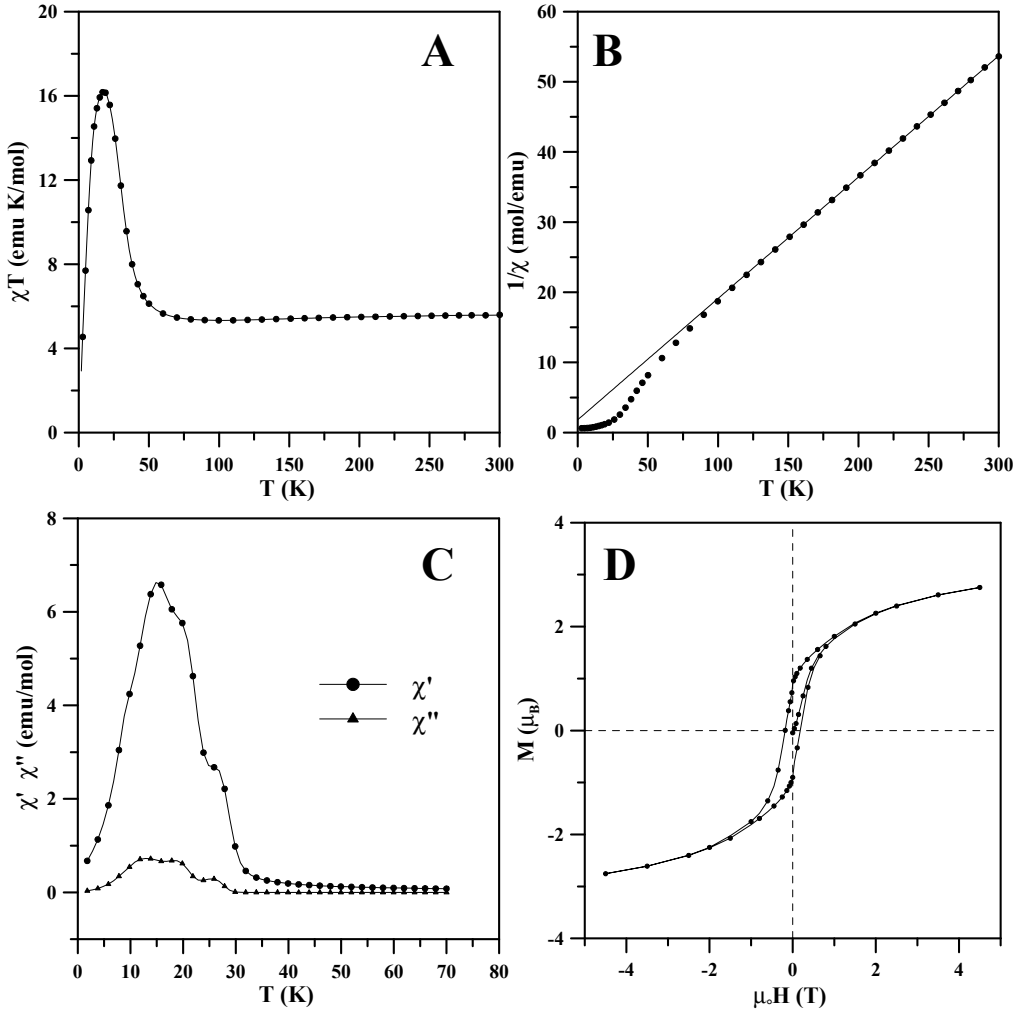

Figure S9: Magnetic characterization of the Co-YVL hybrids: (A) χT as a function of temperature, (B) Inverse of χ as a function of temperature, (C) Magnetic susceptibility as a function of temperature in an ac field, and (D) Field dependant magnetization at 1.8 K.

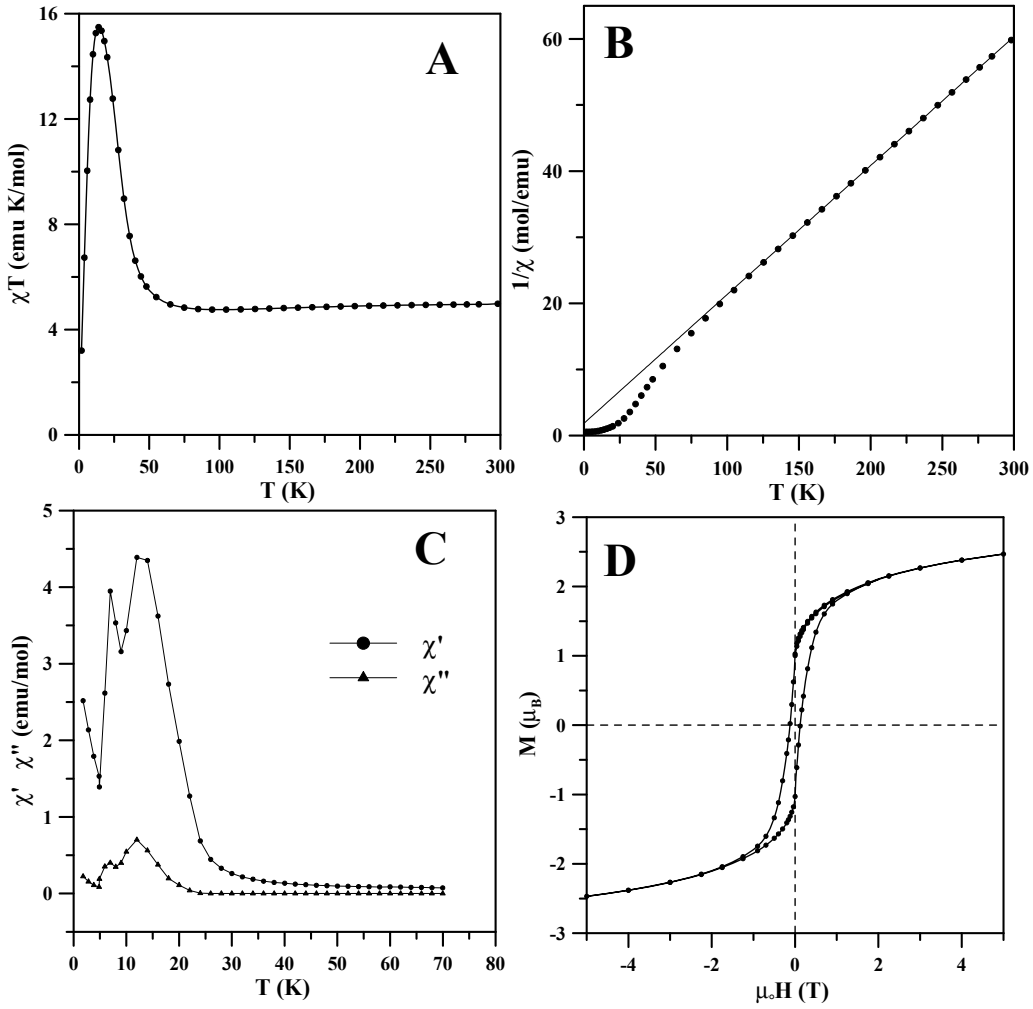

Figure S10: Magnetic characterization of the Co-FVL hybrids: (A) χT as a function of temperature, (B) Inverse of χ as a function of temperature, (C) Magnetic susceptibility as a function of temperature in an ac field, and (D) Field dependant magnetization at 1.8 K.

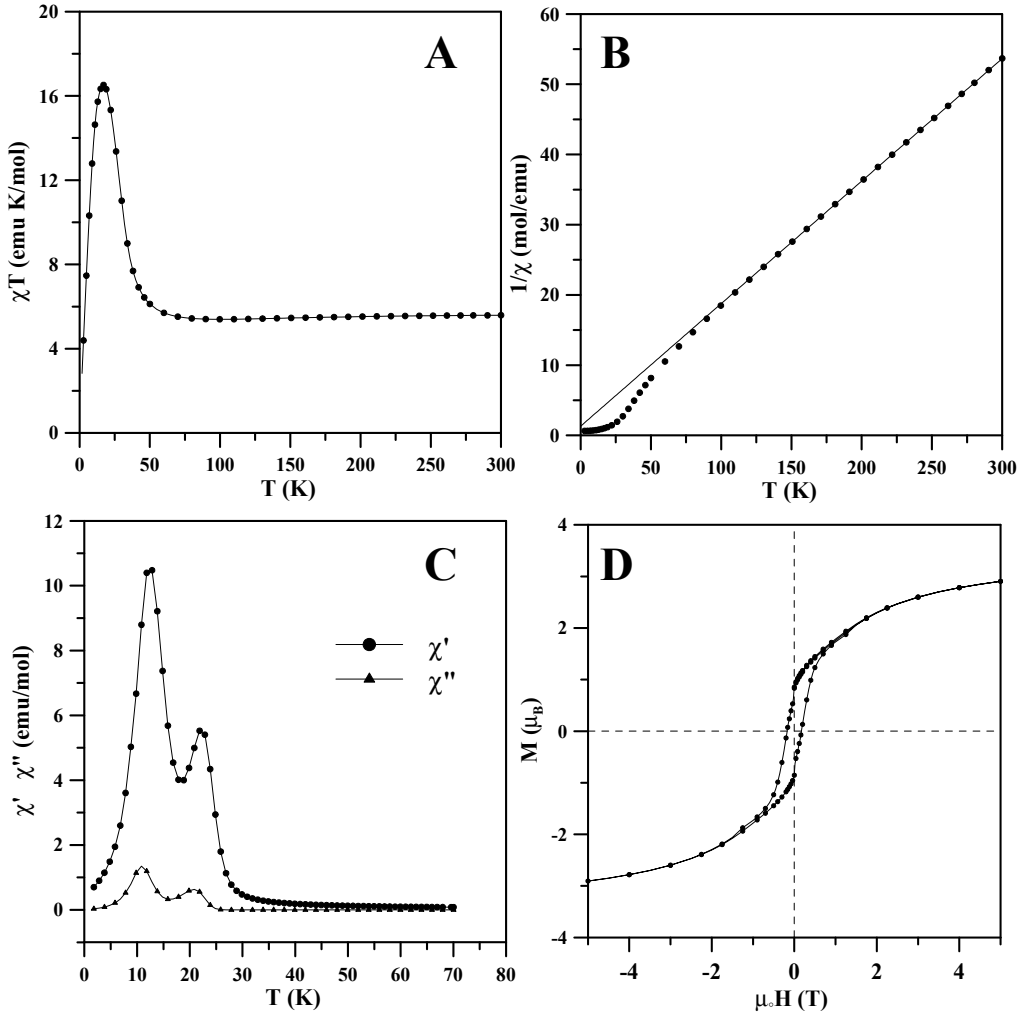

Figure S11: Magnetic characterization of the Co-YVLV hybrids: (A) χT as a function of temperature, (B) Inverse of χ as a function of temperature, (C) Magnetic susceptibility as a function of temperature in an ac field, and (D) Field dependant magnetization at 1.8 K.

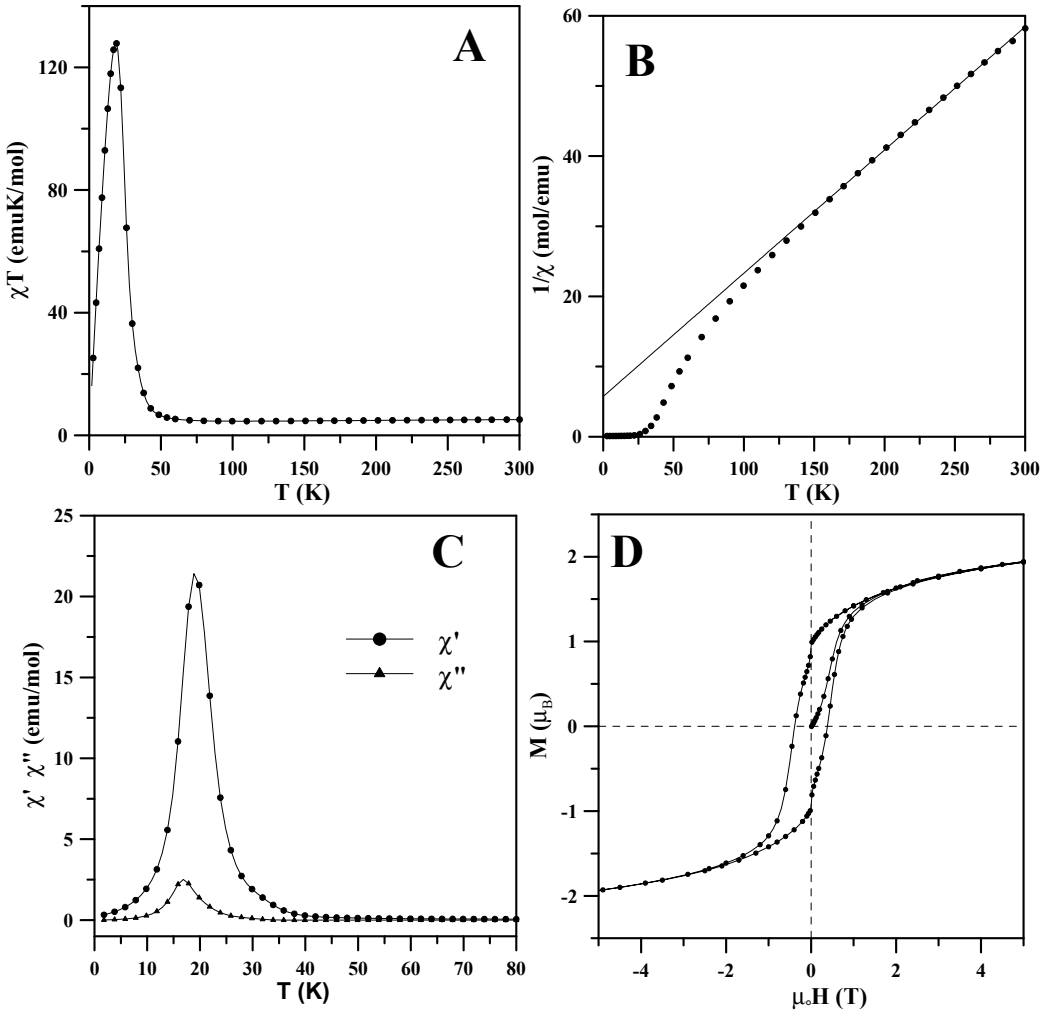

Figure S12: Magnetic characterization of the Co-VVD hybrids: (A) χT as a function of temperature, (B) Inverse of χ as a function of temperature, (C) Magnetic susceptibility as a function of temperature in an ac field, and (D) Field dependant magnetization at 1.8 K.

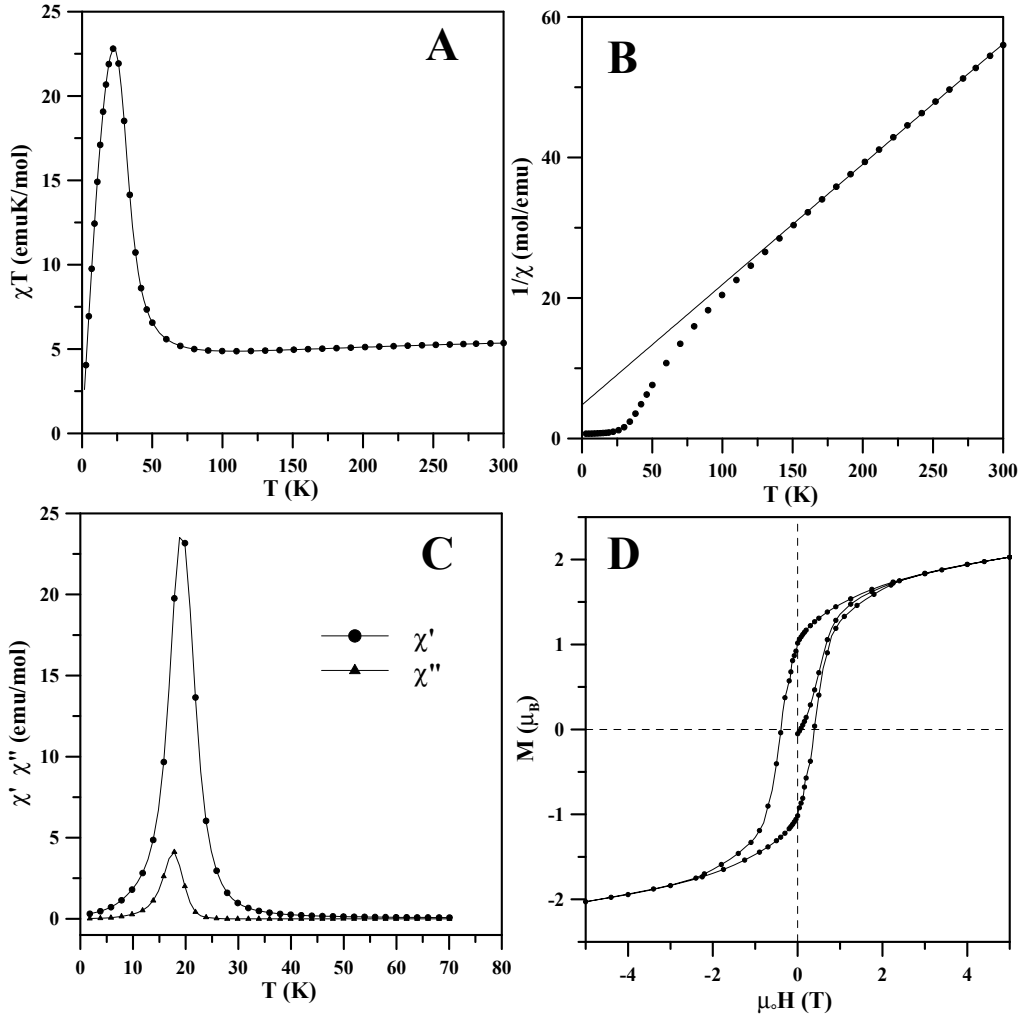

Figure S13: Magnetic characterization of the Co-VVE hybrids: (A) χT as a function of temperature, (B) Inverse of χ as a function of temperature, (C) Magnetic susceptibility as a function of temperature in an ac field, and (D) Field dependant magnetization at 1.8 K.